Available online at www.sciencedirect.com
SCIENCE DIRECT
Journal of Catalysis 228 (2004) 386–396
JOURNAL OF CATALYSIS
www.elsevier.com/locate/jcat

Efficient heterogeneous catalytic systems for enantioselective hydrogenation of prochiral carbonyl compounds

Anirban Ghosh, Rajiv Kumar *

Catalysis Division, National Chemical Laboratory, Pune 411 008, India

Received 6 May 2004; revised 25 August 2004; accepted 31 August 2004
Available online 27 October 2004

Abstract

A proficient heterogeneous catalyst system for stereoselective hydrogenation of carbonyl compounds was synthesized, involving anchoring of Ru^{II}–phosphine–diamine complexes on the inner surfaces of organo-functionalized mesoporous MCM-41 and MCM-48 materials. Powder XRD and TEM experiments reveal highly ordered hexagonal and cubic patterns of the organically modified MCM-41 and MCM-48 materials, respectively, even after incorporation of Ru complexes. Moreover, the integrity of the Ru complexes was retained after anchoring into the mesoporous hosts, which was supported from FTIR, ^{31}P CP MAS NMR, and XPS analyses. This new heterogeneous catalyst shows promising activity and selectivity in the enantioselective hydrogenation of prochiral ketones. The effects of reaction time, temperature, and hydrogen pressure on the catalytic activity and enantioselectivity were studied in detail. As high as 95–99% ee could be obtained using these solid catalysts under heterogeneous reaction conditions. The anchored solid catalysts can be recycled effectively and reused several times without any loss in activity and selectivity.

Keywords: Heterogeneous catalysis; Organo-functionalization; Mesoporous materials; Ru–phosphine–diamine complex; Heterogenization; Enantioselectivity; Hydrogenation

1. Introduction

The synthesis of enantiomerically pure chiral compounds has fascinated researchers because of its immense importance in the synthesis of fine chemicals, pharmaceuticals, agrochemicals, and fragrance chemicals [1]. An explosive research in this area has been inspired by the fact that the undesired enantiomer of a chiral compound could be a toxin in some biological processes, whose detrimental effects can outdo the vitalities of the desired enantiomer [2,3].

Enantioselective reduction of prochiral ketones to corresponding chiral alcohols, involving molecular dihydrogen and catalytic amounts of transition metal complexes, is quite important from both fundamental and industrial application viewpoints [4–7]. Although, Wilkinson's Ru^{II}–phosphine complexes are well recognized to catalyze hydrogenation of olefins, such catalysts are normally not very active for hydrogenation of carbonyl groups. However, the activity can be remarkably enhanced with the addition of stoichiometric amounts of ethylenediamine [8,9], which decelerates hydrogenation of C=C bonds and in turn accelerates C=O hydrogenation by a "metal–ligand bifunctional catalysis" (MLBC) mechanism [10,11]. This concept, established by Noyori et al., was successfully applied toward hydrogenation of prochiral ketones by using Ru^{II}–chiral-diphosphine–chiral-diamine species as a soluble catalyst in the organic phase [4,10–12]. Appropriate enantiomers of 2,2′-bis(diphenylphosphino)-1,1′-binaphthyl (BINAP) and 1,2-diphenylethylenediamine (DPEN) as the above-noted chiral ligands (coordinated to Ru^{II}) are widely used nowadays in the production of various specialty chemicals [4].

While several attempts have been made to heterogenize the soluble transition metal complex catalysts for a variety of reactions to overcome the disadvantages inherent to homogeneous catalytic systems [13–15], there has been lim-

* Corresponding author. Fax: +91 20 2589 3761.
E-mail address: rajiv@cata.ncl.res.in (R. Kumar).

0021-9517/$ – see front matter
doi:10.1016/j.jcat.2004.08.040

ited success in the case of asymmetric heterogeneous catalysis [16]. Moreover, homogeneous catalysts are characterized by high activity and selectivity, which are not generally achieved by the corresponding heterogeneous catalysts [17–19]. However, recent studies have revealed that some heterogenized catalysts indeed can give equivalent or higher selectivity and yields compared to their homogeneous counterparts [20–22].

Surface modification of M41S-type mesoporous materials, having high surface areas ($> 1000\ m^2\ g^{-1}$) and easily accessible pores (diameter 20–100 Å), by organic functional groups [23,24] has fascinated researchers owing to its immense importance in developing newer strategies for immobilization of catalytically reactive species [15,25], and hence, can be one of the appropriate choices for immobilization of Ru^{II}–phosphine complexes.

Here we report the synthesis, characterization, and catalytic applications of new heterogeneous catalytic systems for enantioselective hydrogenation of carbonyl compounds. We have used a postsynthetic grafting method (followed by covalent tethering) for organo-functionalization of the inner surfaces of MCM-41 and MCM-48, and thereafter heterogenized Ru^{II}–phosphine or Ru^{II}–diphosphine complexes on those surface-modified MCM-41 and MCM-48 materials. These new heterogeneous catalyst systems were characterized by powder XRD, FTIR spectroscopy, ICP-AES analyses, N_2 adsorption measurements, ^{31}P CP MAS NMR spectroscopy, XPS, and TEM experiments, which reveal that the integrity of the mesoporous supports and the Ru^{II} complexes was retained after the immobilization process. Applying these heterogeneous catalysts, we have obtained excellent enantioselectivity in the hydrogenation of prochiral ketones. Acting as a true heterogeneous catalyst, it shows comparable activity and selectivity even after four recycles without any leaching of the Ru complex from the support. The Ru complexes were also grafted onto the organically modified surfaces of amorphous (fumed) silica for comparison of activity and selectivity in hydrogenation reactions, where considerable leaching of ruthenium from fumed silica supports was observed after the reactions.

2. Experimental

2.1. Materials

$RuCl_3 \cdot xH_2O$, (*S*,*S*)-1,2-diphenylethylenediamine (SDPEN), (*S*)-2,2′-bis(diphenylphosphino)-1,1′-binaphthyl [(*S*)-BINAP], *N*-[3-(trimethoxysilyl)propyl]-ethylenediamine (TPEN), 3-chloropropyltrimethoxy silane (CPTS), fumed silica (surface area $= 384\ m^2\ g^{-1}$), dichlorodiphenylsilane (Ph_2SiCl_2), acetophenone, *p*-methylacetophenone, *p*-chloroacetophenone, *p*-methoxyacetophenone, propiophenone, cyclohexylmethylketone, and cyclobutylphenylketone were purchased from Aldrich. Cetyltrimethylammonium bromide (CTABr), triethylamine (NEt_3), ethylmethylketone, potassium *tert*-butoxide (^tBuOK), and 2-propanol were purchased from Loba Chemie, India, and were used as received without further purification.

2.2. Syntheses of parent and organo-functionalized MCM-41 and MCM-48

Initial molar gel compositions of the syntheses mixture of MCM-41 and MCM-48 were SiO_2–0.32 NaOH–0.2 CTABr–125 H_2O and SiO_2–0.4 NaOH–0.21 CTABr–120 H_2O, respectively. In a typical synthesis, fumed silica (3 g) was added to a solution of x g of NaOH [$x = 0.64$ (MCM-41), 0.8 (MCM-48)] in 25 mL H_2O and stirred for 1 h. To this mixture, a solution of y g of CTABr [$y = 3.64$ (MCM-41), 3.82 (MCM-48)] in 50 mL H_2O was added dropwise and stirred for another 1 h. Finally z mL of H_2O [$z = 37$ (MCM-41), 33 (MCM-48)] was added to the synthesis gel, stirred further for 30 min, and autoclaved at 100 °C for 16 h (MCM-41), and at 150 °C for 36 h (MCM-48). All the as-synthesized mesoporous samples were air-calcined at 540 °C for 10 h.

Surface modification of MCM-41 and MCM-48 materials was achieved by a postsynthesis grafting method [23]. One gram of the calcined MCM-41 or MCM-48 materials was suspended in 30 mL of dry dichloromethane (DCM), and first treated with 0.03 mL of dichlorodiphenylsilane (Ph_2SiCl_2) for 1 h under inert conditions to passivate the silanol groups on the external surface by silylation [26]. By this method the tethering of desired organic functional groups is expected to occur predominantly inside the channels [26]. The contents were then cooled to liquid N_2 temperature and 1 mL of the desired trialkoxyorganosilane (TPEN or CPTS) was added dropwise to this slurry. The temperature was gradually increased to 40 °C and the reaction mixture was further stirred for 24 h under inert atmosphere, filtered, washed several times with dry DCM, and dried under vacuum. The resultant ethylenediamine- and chloro-functionalized mesoporous materials thus obtained were designated as EN-MCM-41/48 and Cl-MCM-41/48, respectively.

2.3. Anchoring of $RuCl_2(PPh_3)_3$ and Ru–(*S*)-BINAP complexes inside ethylenediamine-functionalized MCM-41 and MCM-48

The $RuCl_2(PPh_3)_3$ complex was synthesized applying a published procedure [27]. One gram of EN-MCM-41 or EN-MCM-48 was added to a solution containing 38 mg (0.04 mmol) of the $RuCl_2(PPh_3)_3$ complex dissolved in 30 mL of dry DCM, and the mixture was stirred at room temperature for 12 h under inert atmosphere, filtered, washed with dry DCM, and dried under vacuum. The resultant material was designated as RuP-EN-MCM-41/48 (Scheme 1A).

The $[Ru(benzene)Cl_2]_2$ complex was synthesized applying a published procedure [28]. One gram of the EN-MCM-41/48 sample was treated with 30 mg (0.06 mmol) of the

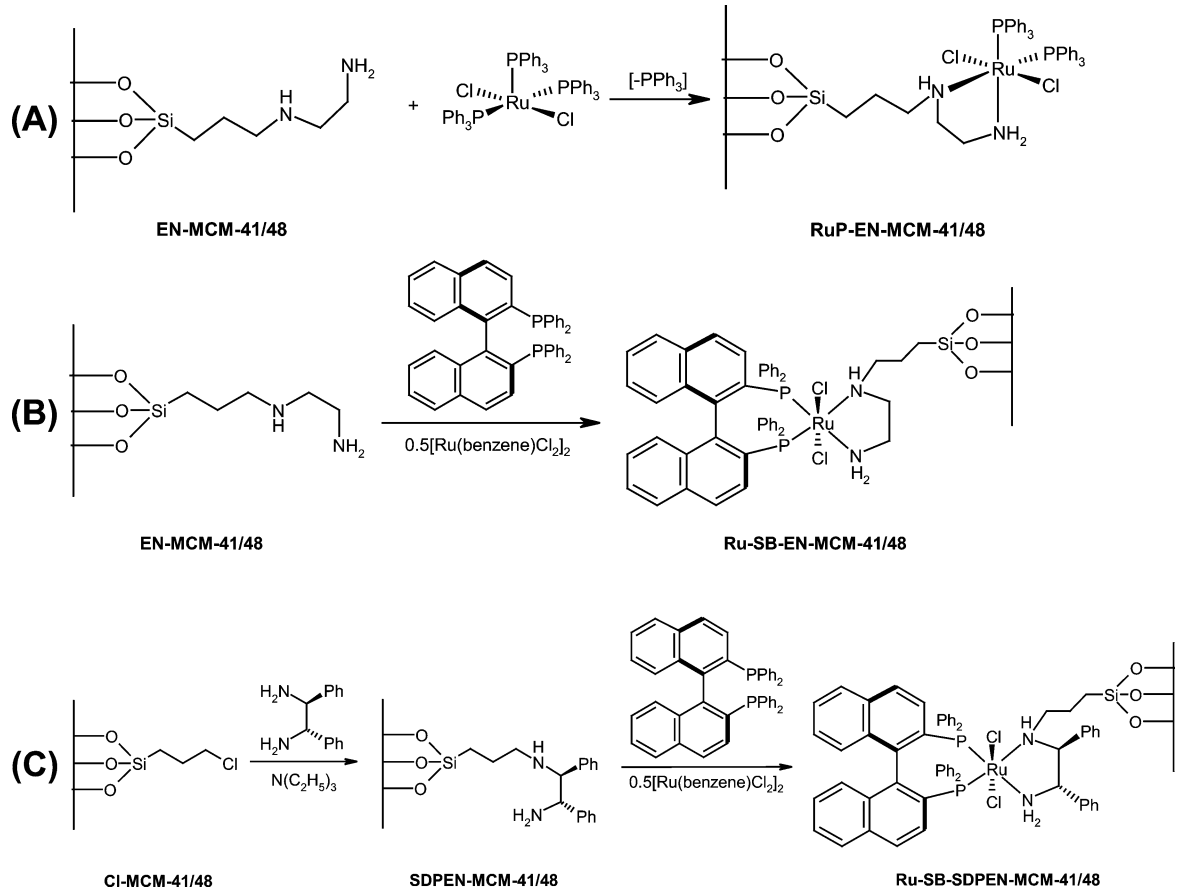

Scheme 1. (A) Immobilization of $RuCl_2(PPh_3)_3$ complex onto ethylenediamine-functionalized MCM-41 and MCM-48. (B) Immobilization of Ru–(*S*)-BINAP complex inside ethylenediamine-functionalized MCM-41 and MCM-48. (C) Covalent tethering of SDPEN on chloro-functionalized MCM-41 and MCM-48, and immobilization of Ru–(*S*)-BINAP complex on the resultant SDPEN-MCM-41 and SDPEN-MCM-48 materials.

$[Ru(benzene)Cl_2]_2$ complex and 75 mg (0.12 mmol) of (*S*)-2,2′-bis(diphenylphosphino)-1,1′-binaphthyl [(*S*)-BINAP or SB] dissolved in 30 mL of dry DCM and refluxed for 12 h under N_2 atmosphere, filtered, washed with dry DCM, and dried under vacuum. The resultant material was designated as Ru–SB-EN-MCM-41/48 (Scheme 1B).

2.4. Grafting of (S,S)-1,2-diphenylethylenediamine (SDPEN) inside chloro-functionalized MCM-41 and MCM-48, and anchoring of Ru–(S)-BINAP complex

A chiral diamine moiety was introduced into the inner surfaces of MCM-41 and MCM-48 via a nucleophilic substitution mechanism (Scheme 1C). The chiral diamine compound chosen here was (*S,S*)-1,2-diphenylethylenediamine. One gram of chloro-functionalized MCM-41 or MCM-48 (Cl-MCM-41/48) was added to a solution containing 106 mg (0.5 mmol) of SDPEN and 0.14 mL of triethylamine (NEt_3) in 30 mL of dry methanol, refluxed for 24 h under inert conditions, filtered, washed with a methanol–water mixture and then with methanol, and dried under vacuum. The resultant material was designated as SDPEN-MCM-41/48.

One gram of the SDPEN-MCM-41/48 material was treated with 30 mg (0.06 mmol) of $[Ru(benzene)Cl_2]_2$ complex and 75 mg (0.12 mmol) of (*S*)-BINAP (SB) dissolved in 30 mL of dry DCM and refluxed for 12 h under N_2 atmosphere, filtered, washed with dry DCM, and dried under vacuum. The resultant material was designated as Ru–SB–SDPEN-MCM-41/48 (Scheme 1C).

2.5. Grafting of different Ru complexes on surfaces of amorphous silica

The surfaces of amorphous silica were also organically modified according to the following procedure. One gram of fumed silica was suspended in 30 mL of dry DCM, and to this either 1 mL of TPEN or 1 mL of CPTS was added dropwise. The reaction mixture was stirred for 24 h under inert atmosphere and reflux conditions, filtered, washed several times with dry DCM, and dried under vacuum to obtain the respective organo-functionalized silica materials designated as EN–SiO_2 or Cl–SiO_2, respectively.

Further, 1 g of the Cl–SiO_2 material was added to a solution containing 106 mg (0.5 mmol) of SDPEN and 0.14 mL of triethylamine (NEt_3) in 30 mL of dry methanol, refluxed for 24 h under inert conditions, filtered, washed with a methanol–water mixture and then with methanol, and dried

under vacuum. The resultant material was designated as SDPEN–SiO_2.

The $RuCl_2(PPh_3)_3$ and Ru–(*S*)-BINAP complexes were anchored on EN–SiO_2 and SDPEN–SiO_2 materials by similar methods as in the case of MCM-41 or MCM-48 (Scheme 1). The resultant materials were designated as RuP–EN–SiO_2, Ru–SB–EN–SiO_2, and Ru–SB–SDPEN–SiO_2, respectively.

2.6. Catalytic hydrogenation reactions

The catalytic hydrogenation reactions of different prochiral aliphatic, alicyclic, and aromatic ketones were performed in a 100 mL high-pressure autoclave at temperatures ranging from 80 to 120 °C, H_2 pressure ranging from 0.34 to 2.76 MPa, stirring speed 500 rpm, and for different durations ranging from 1 to 6 h. One hundred milligrams of the solid catalyst, potassium *tert*-butoxide as the base, and 2-propanol as solvent were used in each reaction. Thereafter, the catalysts were recovered from the hot reaction mixtures by filtration and recycled four times for hydrogenation of the same substrates under identical conditions.

2.7. Characterization techniques

Powder XRD patterns were recorded at room temperature on a Rigaku D Max III VC instrument with Ni-filtered Cu-K_α radiation ($\lambda = 1.5404$ Å), in the 2θ range 1.5–10° at a scan rate of 1° min^{-1}. The specific surface areas of the samples were determined by the BET method from N_2 adsorption isotherms at 77 K using an Omnisorb CX-100 Coulter instrument. Prior to the adsorption experiments, the samples were activated at 150 °C for 6 h at 1.333×10^{-2} Pa. The FTIR spectra were recorded at diffuse reflectance mode on a Perkin–Elmer Spectrum One spectrophotometer operated at a resolution of 4 cm^{-1}. The ^{31}P CP MAS NMR spectra were recorded at 11.7 T and 202.64 MHz in a Bruker DRX-500 FT NMR spectrophotometer. XPS analyses of the catalysts before and after hydrogenation reactions were recorded on a VG Microtech ESCA 3000 spectrometer using unmonochromatized Mg-K_α radiation (photon energy = 1253.6 eV) at a pressure better than 0.133 μPa, pass energy of 50 eV, and electron take-off angle of 60°. TEM images of the samples were recorded on a Jeol Model 1200 EX instrument operated at an accelerating voltage of 100 kV.

The reaction mixtures were analyzed by an Agilent 6890 series gas chromatograph (GC) containing a chiral capillary column (10% permethylated β-cyclodextrin, 30 m × 0.32 mm × 0.25 μm film thickness) and flame ionization detector. The enantiomeric excess (ee) values were determined quantitatively from integration of peak areas in the chromatogram. The products were also confirmed by GC–mass spectroscopy (GCMS) on a Shimadzu GCMS-QP 2000A instrument. The absolute configuration of the products was determined after chemical separation of the enantiomers, by measuring the optical rotation of the individual enantiomers on a JASCO DIP-1020 digital polarimeter and comparing with the literature [29,30]. Further, the separated enantiomers were also analyzed by GC to confirm their respective retention time and quantification.

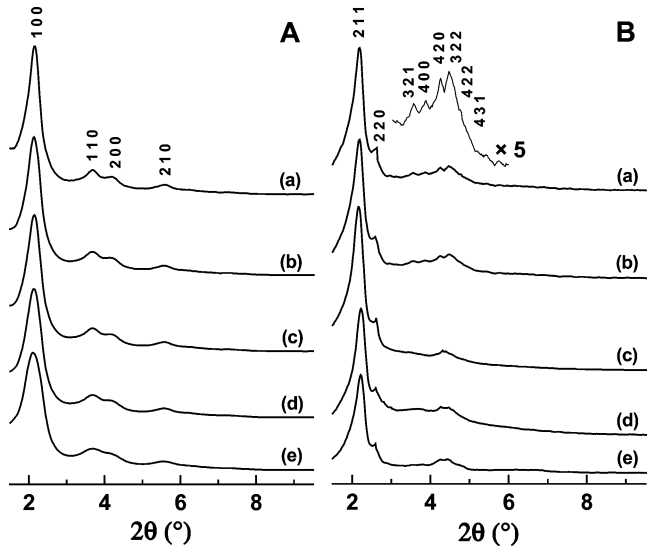

Fig. 1. Powder XRD patterns of the (A) (a) EN-MCM-41, (b) SDPEN-MCM-41, (c) RuP–EN-MCM-41, (d) Ru–SB–EN-MCM-41, and (e) Ru–SB–SDPEN-MCM-41 materials; and (B) (a) EN-MCM-48, (b) SDPEN-MCM-48, (c) RuP–EN-MCM-48, (d) Ru–SB–EN-MCM-48, and (e) Ru–SB–SDPEN-MCM-48 materials.

Inductively coupled plasma–atomic emission spectroscopic (ICP-AES) analyses of the catalysts before and after reactions and the reaction mixtures after filtration of the catalysts were performed on a Perkin–Elmer 1200 inductively coupled plasma spectrophotometer.

3. Results and discussion

3.1. Powder X-ray diffraction

Fig. 1A shows the powder X-ray diffraction (XRD) patterns recorded from (a) EN-MCM-41, (b) SDPEN-MCM-41, (c) RuP-EN-MCM-41, (d) Ru–SB-EN-MCM-41, and (e) Ru–SB–SDPEN-MCM-41 materials. The typical hexagonal phase (*p6mm*) of MCM-41 [main (100) peak with weak (110), (200), and (210) reflections] is clearly visible in all the samples. Fig. 1B shows the XRD patterns of the (a) EN-MCM-48, (b) SDPEN–MCM-48, (c) RuP–EN-MCM-48, (d) Ru–SB-EN-MCM-48, and (e) Ru–SB–SDPEN-MCM-48 materials, in which the strong (211) and (220) reflections along with the weak (321), (400), (420), (322), (422), and (431) reflections are observed in all the materials, characteristic of the cubic phase (*Ia3d*) of MCM-48. These results indicate ordered mesoporosity even after incorporation of organic functional groups and Ru complexes. However, a slight decrease in the peak intensities was observed in the case of the Ru complex loaded samples, which might be due

Table 1
Physical characteristics of the organo-functionalized MCM-41 and MCM-48 materials before and after anchoring of $RuCl_2(PPh_3)_3$ and Ru–(*S*)-BINAP complexes

Materials	% Ru[a] (w/w)	d_{hkl}[b] (Å)	a_0[c] (Å)	Pore diameter (Å)	Pore volume ($cm^3\ g^{-1}$)	Surface area ($m^2\ g^{-1}$)
EN-MCM-41	–	41.05 (100)	47.40	28.43	1.06	993
RuP–EN-MCM-41	0.309	41.15 (100)	47.52	28.39	0.90	864
Ru–SB–EN-MCM-41	0.329	41.79 (100)	48.25	28.42	0.83	824
Cl-MCM-41	–	40.11 (100)	46.31	29.79	1.08	1031
SDPEN-MCM-41	–	40.49 (100)	46.75	29.82	0.93	877
Ru–SB–SDPEN-MCM-41	0.348	40.83 (100)	47.15	29.75	0.84	828
EN-MCM-48	–	38.12 (211)	93.37	25.40	1.19	1336
RuP–EN-MCM-48	0.319	38.67 (211)	94.72	25.31	1.07	1176
Ru–SB–EN-MCM-48	0.351	38.77 (211)	94.97	25.36	0.98	1122
Cl-MCM-48	–	38.92 (211)	95.33	26.93	1.23	1510
SDPEN-MCM-48	–	39.05 (211)	95.65	26.91	1.06	1268
Ru–SB–SDPEN-MCM-48	0.335	39.09 (211)	95.75	27.01	0.95	1141
RuP–EN–SiO_2	0.327	–	–	–	–	n.d.[d]
Ru–SB–EN–SiO_2	0.345	–	–	–	–	n.d.
Ru–SB–SDPEN–SiO_2	0.329	–	–	–	–	n.d.

[a] Analyzed from ICP-AES.
[b] Calculated from XRD patterns ($n\lambda = 2d\sin\theta$, where $n = 1$ and $\lambda = 1.5404$ Å). Values in parentheses are respective principal Miller indices.
[c] $a_0 = d_{100} \times 2/\sqrt{3}$ (for MCM-41); $a_0 = d_{211} \times \sqrt{6}$ (for MCM-48).
[d] n.d., not determined.

to partial filling of the void space due to the presence of Ru complexes inside the mesopores.

A comparison of d spacings and unit cell parameter (a_0) values (calculated from XRD patterns) of the functionalized MCM-41 and MCM-48 materials, and those with anchored Ru complexes, is presented in Table 1. The Ru contents in each material (including the Ru complex–SiO_2 composite materials), analyzed by ICP-AES, are also included in Table 1.

3.2. Specific surface area

The specific surface area, pore volume, and pore diameter values (estimated from N_2 adsorption–desorption isotherms) of the functionalized MCM-41 and MCM-48 materials, and those with anchored Ru complexes, are presented in Table 1. In the case of EN-MCM-41 material, ca. 13 and 17% decreases in surface area values were observed after incorporation of $RuCl_2(PPh_3)_3$ and Ru–(*S*)-BINAP complexes, respectively. Similar decreases were observed after anchoring of SDPEN and Ru–(*S*)-BINAP (ca. 15 and 20%, respectively) inside Cl-MCM-41 material. Analogous trends were also observed in the surface area values of the MCM-48 materials, and in the pore volumes of the MCM-41 and MCM-48 materials after anchoring of the Ru complexes. The pore diameter values of these materials, however, did not change considerably after anchoring of the Ru complexes. All these results indicate that partial filling of the mesopores had occurred by the aforesaid complexes, which are anchored inside of the pore structure.

3.3. FTIR spectra

Fig. 2 shows the FTIR spectra of the (A) (a) RuP–EN-MCM-41 and (b) Ru–SB–SDPEN-MCM-41 materials; and (B) (a) RuP–EN-MCM-48 and (b) Ru–SB–SDPEN-MCM-48 materials. Insets show the FTIR spectra of the (A) SDPEN-MCM-41 and (B) SDPEN-MCM-48 materials. The characteristic P–Ph band at ca. 1086 cm^{-1} [31] were observed in the spectra of the RuP–EN-MCM-41/48 and Ru–SB–SDPEN-MCM-41/48 materials, clearly indicating the incorporation of Ru–phosphine complexes. In the case of SDPEN-MCM-41 (inset of Fig. 2A) and SDPEN-MCM-48 (inset of Fig. 2B) materials, the characteristic bands of $–NH_2$ at 3303 and 3365 cm^{-1} and another two bands at 2935 and 2872 cm^{-1} corresponding to asymmetric and symmetric vibrations, respectively, of the $–CH_2$ groups of the propyl chain of the silylating agent were observed, indicative of anchoring of amine moieties in the mesopores.

3.4. ^{31}P CP MAS NMR spectra

The ^1H–^{31}P coupled CP MAS NMR spectra of the (a) RuP–EN-MCM-41, (b) Ru–SB–EN-MCM-41, and (c) Ru–SB–SDPEN-MCM-41 materials are given in Fig. 3. The spectrum of the RuP–EN-MCM-41 material reveals two major ^{31}P signals at $\delta = 36$ and 69 ppm, each split by J coupling to other ^{31}P nuclei (Fig. 3, curve a). The integrated intensity for these major signals is in the ratio 1:1. The $RuCl_2(PPh_3)_3$ molecule has a distorted square pyramidal structure, with the equatorial positions occupied by two PPh_3 groups trans to each other, and two –Cl ligands trans to each other. Another PPh_3 group occupies the axial position (Scheme 1A). This

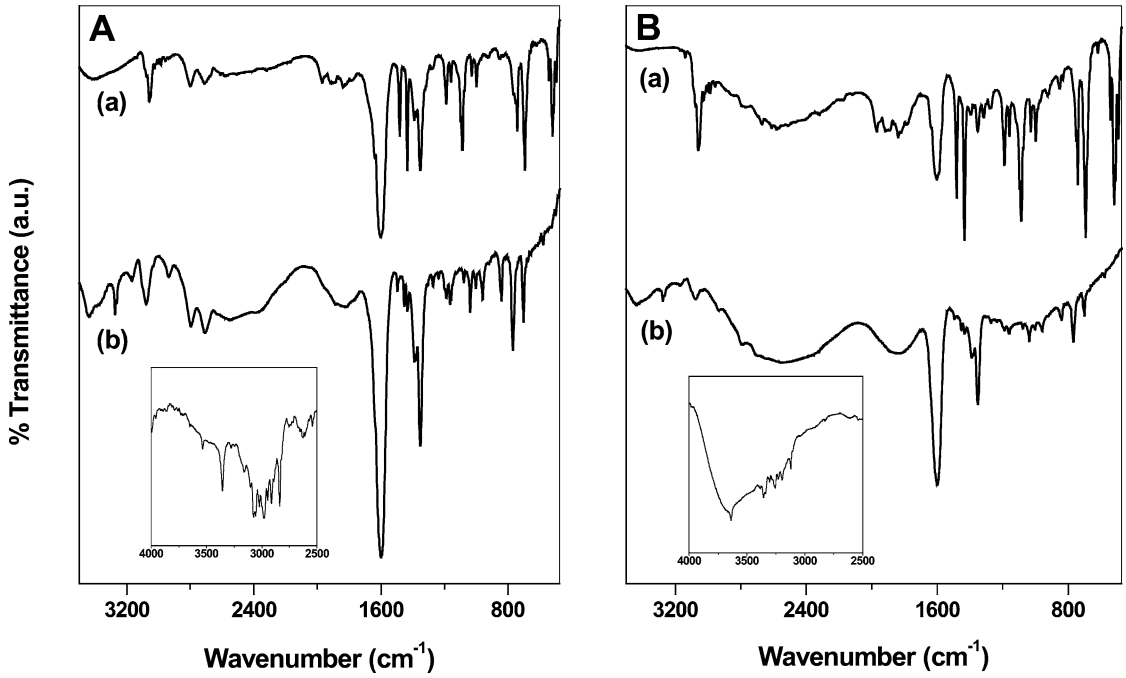

Fig. 2. FTIR spectra of the (A) (a) RuP–EN-MCM-41 and (b) Ru–SB–SDPEN-MCM-41 materials; and (B) (a) RuP–EN-MCM-48 and (b) Ru–SB–SDPEN-MCM-48 materials. Insets represent the FTIR spectra of the (A) SDPEN-MCM-41 and (B) SDPEN-MCM-48 materials.

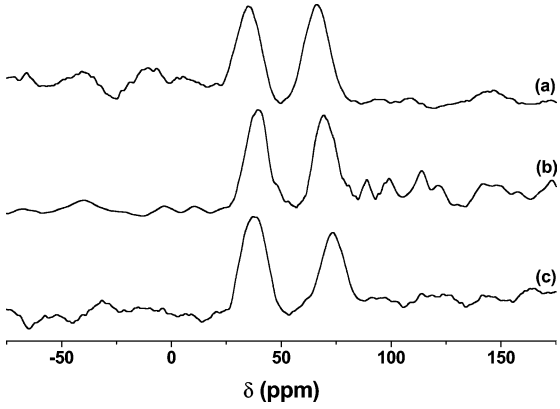

Fig. 3. The ^{1}H–^{31}P coupled CP MAS NMR spectra of the (a) RuP–EN-MCM-41, (b) Ru–SB–EN-MCM-41, and (c) Ru–SB–SDPEN-MCM-41 materials.

makes the central Ru nuclei coordinatively unsaturated. The three phosphorus atoms in $RuCl_2(PPh_3)_3$ may be grouped into (i) one distinct (one PPh_3 group in axial position) and (ii) two equivalent (two PPh_3 groups in equatorial position trans to each other) phosphorus environments (Scheme 1A). On interaction of $RuCl_2(PPh_3)_3$ with the chelating ethylenediamine ligand of the EN-MCM-41 material, one PPh_3 group in the equatorial position leaves the system due to a strong trans effect of another PPh_3 group. Thus, the bidentate ethylenediamine ligand coordinates with the Ru nuclei through (i) the vacant equatorial position created by the PPh_3 group, and (ii) through the already vacant axial position, thus creating two nonequivalent phosphorus environments (Scheme 1A). This mechanism depicted in Scheme 1A is supported by the spectrum of the RuP–EN-MCM-41 material, in which two distinct peaks of almost equal intensity were observed (Fig. 3, curve a), signifying the existence of two nonequivalent phosphorus atoms in the material.

The ^{31}P NMR spectra of the Ru–SB–EN-MCM-41 and Ru–SB–SDPEN-MCM-41 materials (Fig. 3, curves b and c) also show two distinct peaks of approximately equal intensity at $\delta \sim 40$ and 71 ppm, which can also be attributed to the presence of two nonequivalent phosphorus atoms of the BINAP ligand inside the material. The inclusion of the EN and SDPEN moieties on the mesoporous silica surface leads to two nonequivalent phosphorus environments inside the Ru–SB–EN-MCM-41 (Scheme 1B) and Ru–SB–SDPEN-MCM-41 (Scheme 1C) materials, respectively, which accounts for the two strong ^{31}P signals.

3.5. X-ray photoelectron spectra

Additional support for the anchoring of the Ru^{II} complexes onto the solid mesoporous materials was obtained by XPS analyses. Table 2 represents the Ru $3d_{5/2}$, Ru $3p_{3/2}$, N 1s, Si 2p, and P 2p core-level binding energies (BE) obtained from XPS analyses of the EN-MCM-41/48 and SDPEN-MCM-41/48 materials before and after anchoring of $RuCl_2(PPh_3)_3$ and Ru–(*S*)-BINAP complexes, and of the Ru complex–fumed silica composite materials. From the Ru $3d_{5/2}$ and $3p_{3/2}$ BE values at ca. 280 eV and ca. 465 eV, respectively, it is evident that all ruthenium in the catalysts are present as Ru^{II} species [32]. The P 2p BE values are also consistent with those obtained from Ru^{II}–phosphine complexes [32]. This further showed that the integrity of the $RuCl_2(PPh_3)_3$ and Ru–(*S*)-BINAP complexes was retained

Table 2
Core-level binding energies (in eV) of various elements[a] present in the catalyst precursors and the anchored catalysts

Materials	Ru $3d_{5/2}$	Ru $3p_{3/2}$	N 1s	Si 2p	P 2p
EN-MCM-41	–	–	399.4	103.4	–
RuP–EN-MCM-41	280.5	464.8	400.1	103.4	131.3
Ru–SB–EN-MCM-41	280.8	465.0	400.2	103.4	131.5
SDPEN-MCM-41	–	–	400.1	103.4	–
Ru–SB–SDPEN-MCM-41	280.8	465.0	400.7	103.4	131.6
EN-MCM-48	–	–	399.5	103.4	–
RuP–EN-MCM-48	280.5	464.9	400.2	103.4	131.3
Ru–SB–EN-MCM-48	280.7	465.0	400.3	103.4	131.4
SDPEN-MCM-48	–	–	400.0	103.4	–
Ru–SB–SDPEN-MCM-48	280.7	465.0	400.6	103.4	131.5
RuP–EN–SiO_2	280.6	464.8	400.3	103.3	131.4
Ru–SB–EN–SiO_2	280.8	464.9	400.3	103.3	131.5
Ru–SB–SDPEN–SiO_2	280.8	464.9	400.5	103.3	131.6

[a] The core-level binding energies were aligned with respect to the C 1s binding energy of 285 eV using adventitious carbon.

when anchored into the supports, with no beam damage suffered by the supports.

The N 1s BE values in the EN-MCM-41/48 and SDPEN-MCM-41/48 materials indeed confirm successful grafting of amine moieties inside the mesopores, previously inferred from FTIR spectra (insets of Fig. 2). However, an increase in N 1s BE values by ca. 0.6–0.7 eV was observed after loading of the Ru complexes in each material, which can be attributed to coordination of N atoms with the Ru^{II} nuclei. All these results strongly support the stable anchoring and immobilization of $RuCl_2(PPh_3)_3$ and Ru–(*S*)-BINAP complexes onto the surface of MCM-41 and MCM-48 mesoporous materials.

3.6. Transmission electron microscopy

Fig. 4 represents TEM images recorded from (A) RuP–EN-MCM-41, (B) Ru–SB–SDPEN-MCM-41, (C) RuP–EN-MCM-48, and (D) Ru–SB–SDPEN-MCM-48. The selected area electron diffraction (SAED) patterns of the samples shown in Figs. 4B and 4D are given in Figs. 4E and 4F, respectively. The TEM images and SAED patterns are well consistent with the regular hexagonal and cubic mesophases of MCM-41 and MCM-48, respectively, with homogeneity in patterns throughout, which indicates the retention of ordered patterns of MCM-41 and MCM-48 even after anchoring of the above-noted Ru^{II}–phosphine complexes, further corroborating the XRD results (Fig. 1).

3.7. Enantioselective hydrogenation of prochiral ketones

All the heterogeneous catalysts prepared in this study were exploited in the enantioselective hydrogenation of prochiral aliphatic, alicyclic, and aromatic ketones, and the results are summarized in Table 3 (for aliphatic and alicyclic ketones) and Table 4 (for aromatic ketones). Similar reactions were also performed with the pure Ru–SB–SDPEN

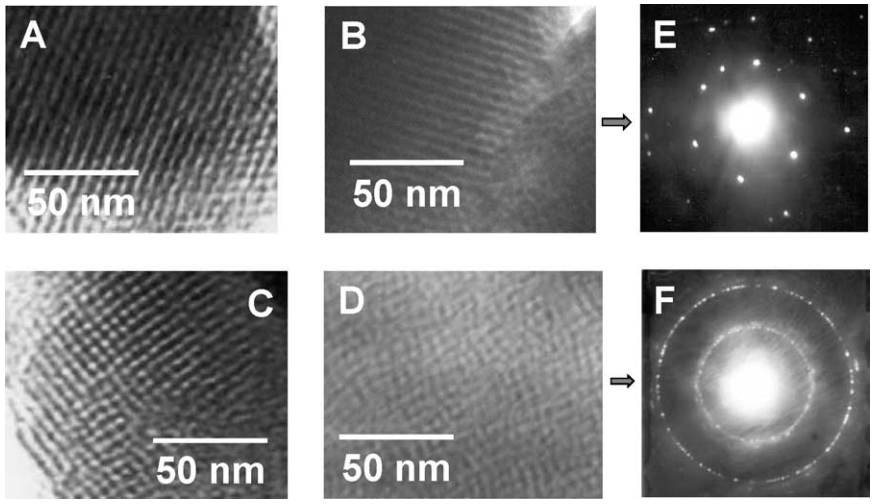

Fig. 4. TEM images of the (A) RuP–EN-MCM-41, (B) Ru–SB–SDPEN-MCM-41, (C) RuP–EN-MCM-48, and (D) Ru–SB–SDPEN-MCM-48. (E) and (F) show the SAED patterns of the samples shown in (B) and (D), respectively.

Table 3
Enantioselective hydrogenation[a] of prochiral aliphatic and alicyclic ketones

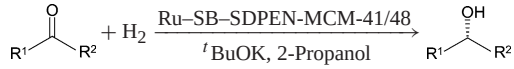

Entry	Catalyst	Substrate	Conversion[b] (mol%)	TOF[c] (h^{-1})	ee (%)
1	RuP–EN-MCM-41	$R^1 = C_2H_5$, $R^2 = CH_3$	91	515	16
2	Ru–SB–EN-MCM-41	$R^1 = C_2H_5$, $R^2 = CH_3$	93	495	28
3	Ru–SB–SDPEN-MCM-41	$R^1 = C_2H_5$, $R^2 = CH_3$	96	483	99
4	RuP–EN-MCM-48	$R^1 = C_2H_5$, $R^2 = CH_3$	90	494	14
5	Ru–SB–EN-MCM-48	$R^1 = C_2H_5$, $R^2 = CH_3$	94	469	29
6	Ru–SB–SDPEN-MCM-48	$R^1 = C_2H_5$, $R^2 = CH_3$	97	507	99
7	Ru–SB–SDPEN–SiO_2	$R^1 = C_2H_5$, $R^2 = CH_3$	91	455	90
8	Ru–SB–SDPEN[d]	$R^1 = C_2H_5$, $R^2 = CH_3$	> 99	940	> 99
9	Ru–SB–SDPEN-MCM-41	R^1 = Cyclohexyl, $R^2 = CH_3$	72	362	91
10	Ru–SB–SDPEN-MCM-48	R^1 = Cyclohexyl, $R^2 = CH_3$	79	394	94

[a] Reaction conditions: catalyst = 100 mg; substrate = 7 mmol; substrate:base = 100:1; Ru:substrate = 1:2265 (RuP–EN-MCM-41), 1:2194 (RuP–EN-MCM-48), 1:2128 (Ru–SB–EN-MCM-41), 1:1994 (Ru–SB–EN-MCM-48), 1:2011 (Ru–SB–SDPEN-MCM-41), 1:2089 (Ru–SB–SDPEN-MCM-48), 1:2000 (Ru–SB–SDPEN); temperature = 100 °C; H_2 pressure = 1.38 MPa; stirring speed = 500 rpm; duration = 4 h (heterogeneous), 2 h (homogeneous).
[b] Absolute configuration of all the reaction products is (*S*).
[c] TOF = (mmol of ketone converted to alcohol) × (mmol of Ru)$^{-1}$ × h^{-1}.
[d] Reaction under homogeneous conditions.

Table 4
Enantioselective hydrogenation[a] of prochiral aromatic ketones

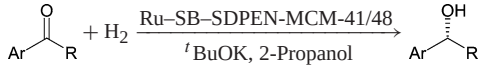

Entry	Catalyst	Substrate	Conversion[b] (mol%)	TOF[c] (h^{-1})	ee (%)
1	RuP–EN-MCM-41	Ar = Ph, R = Me	89	504	18
2	Ru–SB–EN-MCM-41	Ar = Ph, R = Me	92	489	31
3	Ru–SB–SDPEN-MCM-41	Ar = Ph, R = Me	94	472	93
4	RuP–EN-MCM-48	Ar = Ph, R = Me	86	472	22
5	Ru–SB–EN-MCM-48	Ar = Ph, R = Me	91	454	39
6	Ru–SB–SDPEN-MCM-48	Ar = Ph, R = Me	96	501	95
7	Ru–SB–SDPEN–SiO_2	Ar = Ph, R = Me	92	460	94
8	Ru–SB–SDPEN[d]	Ar = Ph, R = Me	> 99	990	> 99
9	Ru–SB–SDPEN-MCM-41	Ar = 4′-Me-Ph, R = Me	95	478	94
10	Ru–SB–SDPEN-MCM-48	Ar = 4′-Me-Ph, R = Me	97	507	96
11	Ru–SB–SDPEN-MCM-41	Ar = 4′-Cl-Ph, R = Me	98	493	96
12	Ru–SB–SDPEN-MCM-48	Ar = 4′-Cl-Ph, R = Me	99	517	98
13	Ru–SB–SDPEN-MCM-41	Ar = Ph, R = Et	95	478	91
14	Ru–SB–SDPEN-MCM-48	Ar = Ph, R = Et	96	501	93
15	Ru–SB–SDPEN-MCM-41	Ar = 4′-MeO-Ph, R = Me	88	442	95
16	Ru–SB–SDPEN-MCM-48	Ar = 4′-MeO-Ph, R = Me	91	475	96
17	Ru–SB–SDPEN-MCM-41	Ar = Ph, R = Cyclobutyl	75	377	91
18	Ru–SB–SDPEN-MCM-48	Ar = Ph, R = Cyclobutyl	79	413	93

[a] Reaction conditions: catalyst = 100 mg; substrate = 7 mmol; substrate:base = 100:1; Ru:substrate = 1:2265 (RuP–EN-MCM-41), 1:2194 (RuP–EN-MCM-48), 1:2128 (Ru–SB–EN-MCM-41), 1:1994 (Ru–SB–EN-MCM-48), 1:2011 (Ru–SB–SDPEN-MCM-41), 1:2089 (Ru–SB–SDPEN-MCM-48), 1:2000 (Ru–SB–SDPEN); temperature = 100 °C; H_2 pressure = 1.38 MPa; stirring speed = 500 rpm; duration = 4 h (heterogeneous), 2 h (homogeneous).
[b] Absolute configuration of all the reaction products is (*S*).
[c] TOF = (mmol of ketone converted to alcohol) × (mmol of Ru)$^{-1}$ × h^{-1}.
[d] Reaction under homogeneous conditions.

complex [9] under homogeneous conditions for comparative purposes.

From the tables, it is evident that all the substrates were hydrogenated with very high conversion (upto 99%) and excellent enantiomeric excess (upto 99%) by the Ru–SB–SDPEN-containing catalysts (Table 3, entries 3, 6–10, and Table 4, entries 3, 6–18). Although, the RuP–EN-MCM-41/48 and Ru–SB–EN-MCM-41/48 catalysts also show similar catalytic activity, they exhibit poor enantioselectivity [ee < 25% (for RuP–EN-MCM-41/48), and < 40% (for Ru–SB–EN-MCM-41/48)]. From these results it is clear that both the biphosphine and the diamine ligands around the central Ru^{II} ion necessarily have to be chiral for maximum enantioselection in agreement with the observations of Noyori et al. [10,11]. Almost comparable activity and enantioselectivity of MCM-41- and MCM-48-based cata-

lysts show that the reaction rate does not essentially depend upon whether the support is MCM-41 or MCM-48, possibly due to a similar rate of interaction between substrate molecules and catalyst active site. Control experiments with the homogeneous Ru–SB–SDPEN complex (entry 8 in Tables 3 and 4) show that reaction is ca. twice faster in homogeneous system vis-à-vis the same complex anchored in MCM-41 and MCM-48. However, the ee was almost comparable. This could be due to a slower rate of interaction between the substrate and the catalyst in the heterogeneous solid–liquid system compared to that in the homogeneous liquid system. In the case of acyclic ethylmethylketone, while the conversion is higher vis-à-vis cyclohexylmethylketone (Table 3, entries 3 and 6 versus 9 and 10), as expected due to relative bulkiness of the substituent group in the vicinity of the carbonyl group, the ee in the case of both the substrates was comparable. A similar trend was also observed in the case of acetophenone and cyclobutylphenylketone (Table 4, entries 3 and 6 versus 17 and 18). However, there was insignificant effect of substitution in the aromatic ring of acetophenone on the conversion as well as ee (Table 4, entries 3, 6, 9–16) in agreement with the results obtained by Hu et al. [18]. The detailed catalytic studies, discussed below, were performed using acetophenone as substrate.

3.7.1. Influence of reaction time

The influence of reaction time over the conversion and enantioselectivity in the hydrogenation of acetophenone is presented in Fig. 5. It was found that for MCM-41- and MCM-48-based heterogeneous catalysts, the conversion increases as the reaction proceeds, as expected, and reaches an optimum value (> 90%) before 4 h time. The enantiomeric excess values, however, attain a maximum from the very beginning of the reactions. For the reaction involving the homogeneous catalyst, the substrate was almost quantitatively hydrogenated at ca. 2 h time. This accounts for the high TOF values in the case of the homogeneous catalyst compared to its heterogeneous counterparts (Tables 3 and 4), expectedly due to restricted interaction between substrate and catalyst under heterogeneous conditions compared to that under homogeneous conditions, as noted above.

3.7.2. Influence of temperature

A critical temperature of 100 °C is required to acquire the activation energy for hydrogenation by the chosen catalyst system, both homogeneous and heterogeneous (Fig. 6). At this temperature the maximum conversion of acetophenone by the Ru–SB–SDPEN-MCM-41/48 catalyst system was achieved. By increasing the temperature to 120 °C, no further change in reaction rate was observed. However, the best ee was obtained at 100 °C; below and above this temperature the ee decreases slightly.

3.7.3. Influence of H_2 pressure

The pressure of molecular hydrogen inside the reaction vessel has a pronounced effect over the conversion. But the enantioselectivity of the heterogeneous catalyst does not significantly depend on the H_2 pressure. As represented in Fig. 7, the conversion of acetophenone markedly increases with H_2 pressure. It was envisaged that maximum conversion of the substrate and ee were achieved at ca. 1.4 MPa pressure, beyond which no further enhancement in reaction rate as well as in ee was experienced.

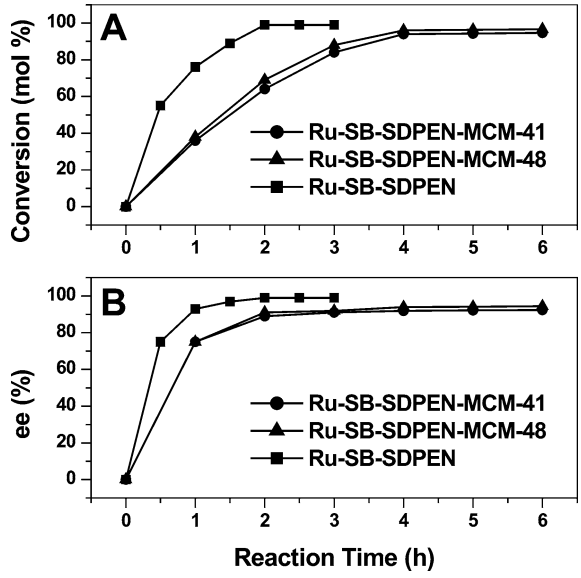

Fig. 5. Influence of reaction time over (A) conversion and (B) enantioselectivity in the hydrogenation of acetophenone by the Ru–SB–SDPEN-MCM-41, Ru–SB–SDPEN-MCM-48, and homogeneous Ru–SB–SDPEN catalysts.

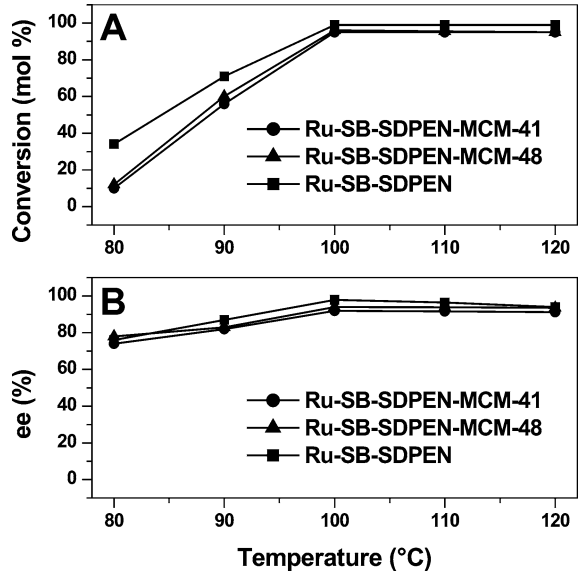

Fig. 6. Influence of temperature over (A) conversion and (B) enantioselectivity in the hydrogenation of acetophenone by the Ru–SB–SDPEN-MCM-41, Ru–SB–SDPEN-MCM-48, and homogeneous Ru–SB–SDPEN catalysts.

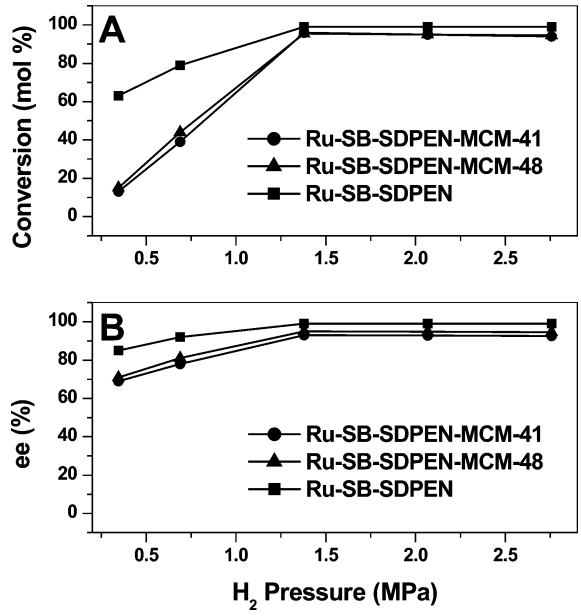

Fig. 7. Influence of H_2 pressure over (A) conversion and (B) enantioselectivity in the hydrogenation of acetophenone by the Ru–SB–SDPEN-MCM-41, Ru–SB–SDPEN-MCM-48, and homogeneous Ru–SB–SDPEN catalysts.

3.7.4. Recycle studies

The stability of the heterogeneous catalysts was evaluated by recovering them from the hot reaction mixtures by filtration, and analyzing the filtrates for Ru content by ICP-AES. In the case of Ru–SB–SDPEN-MCM-41/48 catalysts, the Ru contents in the total filtrate were found to be ca. 1×10^{-3}% of the total Ru present in the catalyst, indicating insignificant leaching of the metal and therefore metal complex. Besides, both of these catalysts were effectively recycled four times for hydrogenation of acetophenone without any significant decline in activity and enantioselectivity (Table 5). In contrast to these, the catalyst prepared by anchoring the Ru–(*S*)-BINAP complex onto SDPEN-functionalized fumed silica (Ru–SB–SDPEN–SiO_2 material) showed a substantial amount of leaching of Ru metal (ca. 26.5% of the total Ru content present in the catalyst used) during reaction in the first cycle, which also leads to a major decrease in catalytic activity and selectivity after four recycles (Table 5).

The stability of the heterogeneous catalysts after hydrogenation reactions was also supported from XPS analyses of the filtered catalysts. The core-level BE of the elements in the recycled MCM-41- and MCM-48-based catalysts (Table 6) match exactly with those in the parent materials before reaction (Table 2), indicating that neither the metal nor the ligands changed their chemical environment during reactions. However, in the case of the Ru–SB–SDPEN–SiO_2 sample, the Ru $3d_{5/2}$ BE could not be evaluated since the core-level spectra merged with the C 1s spectra (Table 6). Moreover, the characteristic Ru $3p_{3/2}$ peak at ca. 465 eV was not observed at all (Table 6) due to insufficient concentration of Ru^{II} species mainly because of significant leaching of the Ru complex from the silica matrix.

4. Summary and conclusions

In conclusion, the synthesis of efficient heterogeneous catalyst systems, by anchoring of $RuCl_2(PPh_3)_3$ and Ru–(*S*)-BINAP complexes inside ethylenediamine- and (*S*,*S*)-

Table 5
Recycle studies of the heterogeneous catalysts for hydrogenation of acetophenone

No. of recycles	Ru–SB–SDPEN–SiO_2		Ru–SB–SDPEN-MCM-41		Ru–SB–SDPEN-MCM-48	
	Conversion (mol%)	ee (%)	Conversion (mol%)	ee (%)	Conversion (mol%)	ee (%)
0	92.0	94	94.0	93	96.0	95
1	78.3	84	93.7	93	95.9	95
2	58.9	72	93.8	93	95.7	95
3	42.3	71	93.5	93	95.8	95
4	20.6	70	93.3	93	95.4	95

Table 6
Core-level binding energies (in eV) of various elements[a] in the recycled heterogeneous catalysts after hydrogenation of acetophenone

Catalysts[b]	No. of recycles	Ru $3d_{5/2}$	Ru $3p_{3/2}$	N 1s	Si 2p	P 2p
Ru–SB–SDPEN-MCM-41	1	280.8	465.0	400.7	103.4	131.6
	2	280.8	465.0	400.7	103.4	131.6
Ru–SB–SDPEN-MCM-48	1	280.7	465.0	400.6	103.4	131.5
	2	280.7	465.0	400.6	103.4	131.5
Ru–SB–SDPEN–SiO_2	1	m[c]	n.d.[d]	400.5	103.3	131.6

[a] The core-level binding energies were aligned with respect to the C 1s binding energy of 285 eV using adventitious carbon.
[b] The catalysts were filtered from hot reaction mixtures, washed thoroughly with 2-propanol and DCM, and thereafter analyzed by XPS.
[c] m, merged with the C 1s core-level spectra, could not be identified separately.
[d] n.d., not detected.

1,2-diphenylethylenediamine-functionalized MCM-41 and MCM-48, for enantioselective hydrogenation of prochiral carbonyl compounds, has been demonstrated. In depth characterization of these new catalyst systems by powder XRD, FTIR, ICP-AES, N_2 adsorption, ^{31}P CP MAS NMR, XPS, and TEM analyses strongly point toward stable immobilization of the Ru^{II} complexes inside the mesoporous matrices. The Ru–(*S*)-BINAP complex anchored on SDPEN-functionalized MCM-41/48 (Ru–SB–SDPEN-MCM-41/48) reveals excellent activity and enantioselectivity. The enantioselectivity of the catalysts does not essentially depend upon the duration of reaction, temperature, and pressure of hydrogen. Both the biphosphine and diamine ligands necessarily have to be chiral to achieve maximum enantioselectivity in the hydrogenation of prochiral ketones. This catalyst system can be recycled effectively and reused several times without any leaching of the metal complex from the support and without any decline in activity and selectivity.

Acknowledgments

A.G. acknowledges Council of Scientific and Industrial research (CSIR), Government of India for a research fellowship. The authors thank a research grant from CSIR networking project CMM0005 on “Catalysis and Catalysts”.

References

[1] A.N. Collins, G.N. Sheldrake, J. Crosby (Eds.), Chirality in Industry: The Commercial Manufacture and Applications of Optically Active Compounds, Wiley, New York, 1997.
[2] R.A. Sheldon, Chirotechnology, Dekker, New York, 1993.
[3] I. Ojima (Ed.), Catalytic Asymmetric Synthesis, second ed., Wiley, New York, 2000.
[4] R. Noyori, (Nobel Lecture 2001) Adv. Synth. Catal. 345 (2003) 15.
[5] J. Halpern, Science 217 (1982) 401.
[6] R. Noyori, Asymmetric Catalysis in Organic Synthesis, Wiley, New York, 1994, Chap. 2, pp. 17–94.
[7] T. Ohkuma, R. Noyori, in: E.N. Jacobsen, A. Pfaltz, H. Yamamoto (Eds.), Comprehensive Asymmetric Catalysis, vol. 1, Springer, Berlin, 1999, pp. 199–246.
[8] T. Ohkuma, H. Ooka, S. Hashiguchi, T. Ikariya, R. Noyori, J. Am. Chem. Soc. 117 (1995) 2675.
[9] T. Ohkuma, H. Ooka, T. Ikariya, R. Noyori, J. Am. Chem. Soc. 117 (1995) 10417.
[10] R. Noyori, T. Ohkuma, Angew. Chem. Int. Ed. 40 (2001) 40.
[11] R. Noyori, M. Yamakawa, S. Hashiguchi, J. Org. Chem. 66 (2001) 7931.
[12] R. Noyori, S. Hashiguchi, Acc. Chem. Res. 30 (1997) 97.
[13] P.N. Liu, P.M. Gu, F. Wang, Y.Q. Tu, Org. Lett. 6 (2004) 169.
[14] T. Ohkuma, H. Takeno, Y. Honda, R. Noyori, Adv. Synth. Catal. 343 (2001) 369.
[15] D.E. De Vos, M. Dams, B.F. Sels, P.A. Jacobs, Chem. Rev. 102 (2002) 3615.
[16] C.E. Song, S. Lee, Chem. Rev. 102 (2002) 3495.
[17] A. Hu, H.L. Ngo, W. Lin, Angew. Chem. Int. Ed. 42 (2003) 6000.
[18] A. Hu, H.L. Ngo, W. Lin, J. Am. Chem. Soc. 125 (2003) 11490.
[19] A. Zsigmond, K. Bogar, F. Nothiesz, J. Catal. 213 (2003) 103.
[20] P. McMorn, G.J. Hutchings, Chem. Soc. Rev. 33 (2004) 108.
[21] R. Raja, J.M. Thomas, M.D. Jones, B.F.G. Johnson, D.E.W. Vaughan, J. Am. Chem. Soc. 125 (2003) 14982.
[22] M.D. Jones, R. Raja, J.M. Thomas, B.F.G. Johnson, D.W. Lewis, J. Rouzaud, K.D.M. Harris, Angew. Chem. Int. Ed. 42 (2003) 4326.
[23] A. Stein, B.J. Melde, R.C. Schroden, Adv. Mater. 12 (2000) 1403.
[24] P. Mukherjee, S. Laha, D. Mandal, R. Kumar, Stud. Surf. Sci. Catal. 129 (2000) 283.
[25] J.M. Thomas, Angew. Chem. Int. Ed. 38 (1999) 3588.
[26] D.S. Shephard, W. Zhou, T. Maschmeyer, J.M. Matters, C.L. Roper, S. Parsons, B.F.G. Johnson, M.J. Duer, Angew. Chem. Int. Ed. 37 (1998) 2719.
[27] F.H. Jardine, Prog. Inorg. Chem. 31 (1984) 265.
[28] M.A. Bennett, A.K. Smith, J. Chem. Soc., Dalton Trans. (1974) 233.
[29] H.C. Brown, B.T. Cho, W.S. Park, J. Org. Chem. 53 (1988) 1231.
[30] K. Nakamura, T. Matsuda, J. Org. Chem. 63 (1998) 8957.
[31] D. Venegas-Yazigi, M. Campos-Vallette, A.B.P. Lever, J. Costamagna, R.O. Latorre, W. Hernandez G., J. Chil. Chem. Soc. 48 (2003) 79.
[32] J.W. Robinson (Ed.), Practical Handbook of Spectroscopy, CRC Press, Boca Raton, FL, 1991, pp. 183–418.